Distributed Enforcement of Phase-Cohesiveness for Frequency Control of Islanded Inverter-Based Microgrids

Madi Zholbaryssov, *Student Member, IEEE*, Alejandro D. Domínguez-García, *Member, IEEE*

***Abstract*—In this paper, we propose a frequency controller for lossless microgrids which achieves a desired active power load sharing while regulating system frequency to some nominal value. The control scheme is based on the slow readjustment of the active power reference of each inverter, i.e., each inverter aims to track a slowly-varying reference that is set sufficiently close to its actual active power injection and moved slowly to reach some desired injection value. This way, the control enforces the trajectory to satisfy the so-called phase-cohesiveness property, i.e., the absolute value of the voltage phase angle difference across electrical lines is smaller than $\frac{\pi}{2}$, which ensures that the system remains stable at all times and the actual active power injections track the slowly-varying reference. We also propose a distributed method to find desired injections, which satisfy the phase-cohesiveness property for tree networks as well as for some cyclic networks. We also discuss implementation aspects of the proposed control scheme and demonstrate its feasibility using a 9-bus microgrid.**

I. Introduction

Microgrids have the potential to facilitate the deployment and effective management of Distributed Energy Resources (DERs); however, achieving stable and reliable operation of microgrids poses new control problems. In this paper, we address one such problem; namely, the microgrid generation control problem, with special emphasis on achieving active power load sharing and frequency regulation.

Microgrid generation control systems typically adopt a hierarchical architecture with multiple control layers; each of these layers has different objectives and timing requirements (see, e.g., [1]–[3]). At the bottom of the hierarchy, there is a purely decentralized primary controller that achieves load power sharing among generators by using only local information, although at the expense of the frequency deviating from the nominal value. In the middle layer, there is a secondary controller that eliminates any frequency deviation from the nominal value by using communications either in a centralized (see, e.g., [1], [3]) or a distributed way (see, e.g., [4]–[7]). At the top of the hierarchy, the so-called tertiary control, also implemented by using communications in a centralized or a distributed fashion, is responsible for optimizing certain longer-term operational criteria, e.g., generation cost [4]. Depending on the size of the microgrid, distributed control systems might provide more practical, reliable and cost-effective solution than centralized counterparts because of the communication and sensing range constraints [6].

Although many approaches in the literature are addressing the microgrid generation control problem, they are often based on linearized models (see, e.g., [6], [7]); large signal models have been adopted in recent papers, which present local stability results valid under small perturbations in the load (see, e.g., [5], [8], [9]). However, large load perturbations are typical of islanded microgrids because of a low load factor and lack of rotating inertia (see, e.g., [2], [10]). Several works attempted to mitigate this issue by incorporating additional energy reserves to increase the rotating inertia of the system (see, e.g., [10], [11]). By contrast, our work aims to achieve desired active power load sharing among inverter-interfaced generators and frequency regulation by designing appropriate controls rather than just increasing the system inertia. We design a controller that results in the absolute value of the voltage phase angle difference across electrical lines to be strictly smaller than $\frac{\pi}{2}$—a property referred to as phase-cohesiveness [12]. One of the main results is to show that enforcing phase-cohesiveness ensures (i) semi-global tracking of the desired injections, and (ii) frequency regulation, provided that such property holds initially and at the equilibrium point that results from the desired injections. The latter condition can be enforced for acyclic and some cyclic topologies by solving an optimal network flow problem with quadratic cost and convex constraints.

This paper extends the results of [13] as follows. In addition to the active power sharing controller, which drives the electrical injections to the desired values, we explain how to execute the controller in a more practical scenario and compute its parameters distributively.

II. Preliminaries

In this section, we present the network power flow and dynamic models for lossless microgrids under frequency-based generation control adopted in this work, and formulate the control objectives to be met.

A. Microgrid Network Power Flow Model

Consider a collection of three-phase inverter-interfaced generators and loads interconnected by a lossless network. The topology of this network can be described by an undirected graph, $\mathcal{G}_p = (\mathcal{V}_p, \mathcal{E}_p)$, with $\mathcal{V}_p = \mathcal{V}_p^{(I)} \cup \mathcal{V}_p^{(L)}$, where $\mathcal{V}_p^{(I)} = \{1, \dots, m\}$ denotes the set of nodes with an inverter, and $\mathcal{V}_p^{(L)} = \{m+1, \dots, n\}$ denotes the set of nodes with a load; and where $\mathcal{E}_p \subseteq \mathcal{V}_p \times \mathcal{V}_p$, with $\{i, j\} \in \mathcal{E}_p$ if nodes i and j are electrically connected. The assumption of having lossless electrical lines is often used in the microgrid literature (see, e.g., [5], [14]), which can be justified by, first, assuming that all lines in microgrid have almost homogeneous resistance-to-inductance ratio, and then, by recovering a lossless model by

M. Zholbaryssov and A. D. Domínguez-García are with the ECE Department of the University of Illinois at Urbana-Champaign, Urbana, IL 61801, USA. E-mail: {zholbar1,aledan}@ILLINOIS.EDU.

means of a linear transformation decoupling lossy and lossless injections (see, e.g., [14, Remark 1]).

Assuming balanced operation, let $v_i^{(A)}(t) = V_i(t)\cos(\omega^* t + \theta_i(t))$, $v_i^{(B)}(t) = V_i(t)\cos(\omega^* t + \theta_i(t) - \frac{2\pi}{3})$, and $v_i^{(C)}(t) = V_i(t)\cos(\omega^* t + \theta_i(t) + \frac{2\pi}{3})$ respectively denote the instantaneous voltage of phase A, B, and C at bus $i \in \mathcal{V}_p$, where ω^* is some nominal frequency, $V_i(t)$ is the instantaneous voltage amplitude, and $\theta_i(t)$ is the phase angle in a coordinate frame rotating with frequency ω^*. Then, assuming all quantities are in per unit (see, e.g., [15]), the active power injected into the network via node $i \in \mathcal{V}_p$ is given by

$$P_i(\theta(t), V(t)) = \sum_{j \in \mathcal{V}} V_i(t) V_j(t) B_{ij} \sin(\theta_i(t) - \theta_j(t)), \quad (1)$$

where $\theta(t) = [\theta_1(t), \ldots, \theta_n(t)]^{\mathrm{T}}$, $V(t) = [V_1(t), \ldots, V_n(t)]^{\mathrm{T}}$, and $B_{ij} = -b_{ij}$, with $b_{ij} < 0$ denoting the susceptance of the line connecting nodes i and j. Let $P_j^{(I)}(t)$ denote the active power generated by the inverter at node $j \in \mathcal{V}_p^{(I)}$, and let $P_l^{(L)}(t) > 0$ denote the active power demanded by the load at node $l \in \mathcal{V}_p^{(L)}$; then,

$$P_i^{(I)}(t) = P_i(\theta(t), V(t)),\ i \in \mathcal{V}_p^{(I)}, \quad (2)$$

$$-P_l^{(L)}(t) = P_l(\theta(t), V(t)),\ l \in \mathcal{V}_p^{(L)}. \quad (3)$$

Define a one-to-one map $\mathbb{I} : \mathcal{E}_p \to \mathbb{R}$ such that every e in the set $\{1, 2, \ldots, |\mathcal{E}_p|\}$ is arbitrarily assigned to exactly one edge $\{i, j\} \in \mathcal{E}_p$, i.e., $\mathbb{I}(\{i, j\}) = e$. Then, if we assign directions to each edge $\{i, j\}$ arbitrarily, e.g., i is taken to be the head and j the tail, we can define a node-to-edge incidence matrix, M, as follows: for each $e = \mathbb{I}(\{i, j\})$, $M_{ie} = 1$, $M_{je} = -1$, and zero otherwise. Then, (2) and (3) can be written in vector form as follows:

$$\begin{bmatrix} P^{(I)}(t) \\ -P^{(L)}(t) \end{bmatrix} = P(\theta(t), V(t)) = M\Gamma(V(t)) f(\theta(t)), \quad (4)$$

where $P(\theta(t), V(t)) = [P_1(\theta(t), V(t)), \ldots, P_n(\theta(t), V(t))]^{\mathrm{T}}$, $P^{(I)}(t) = [P_1^{(I)}(t), \ldots, P_m^{(I)}(t)]^{\mathrm{T}}$, $P^{(L)}(t) = [P_{m+1}^{(L)}(t), \ldots, P_n^{(L)}(t)]^{\mathrm{T}}$, $\Gamma(V(t))$ is a diagonal matrix with entries $\Gamma_{ee}(V(t)) = V_i(t) V_j(t) B_{ij}$, $e = \mathbb{I}(\{i, j\})$, $\{i, j\} \in \mathcal{E}_p$, and $f(\theta(t)) = [f_1(\theta(t)), \ldots, f_{|\mathcal{E}|}(\theta(t))]^{\mathrm{T}}$ with $f_e(\theta(t)) = \sin(\theta_i(t) - \theta_j(t))$.

B. Microgrid Frequency-Based Generation Control

In islanded microgrids, each inverter acts as a voltage source by synthesizing phase voltages of the form $v_i^{(A)}(t) = V_i(t)\cos(\omega^* t + \theta_i(t))$, $v_i^{(B)}(t) = V_i(t)\cos(\omega^* t + \theta_i(t) - \frac{2\pi}{3})$, and $v_i^{(C)}(t) = V_i(t)\cos(\omega^* t + \theta_i(t) + \frac{2\pi}{3})$, and regulating $V_i(t)$ and $\dot{\theta}_i(t)$ via some feedback droop-type controls (see, e.g., [16]). A high-order inverter model, which includes inverter inner control loops, voltage- and frequency-droop controllers, can be simplified into a reduced-order model, where the dynamics associated with the voltage controller, which incorporates the voltage-droop controller and the inverter inner voltage control loop that makes the inverter output voltage track the voltage reference computed by the voltage-droop controller, can be ignored at the time-scale of the frequency controller without compromising modeling fidelity (see, e.g., [17, Section III-C, pp. 826-827], [18, Section 5, p. 14]); thus, the voltage magnitudes at all inverter nodes can be assumed to be fixed, i.e., $V_i(t) = V_i$, $i \in \mathcal{V}_p^{(I)}$, for all t. We also assume that microgrid is equipped with some active or passive shunt compensators or some control mechanisms at the load buses, which help to keep the voltages within the limits, and that voltage controllers at the inverter buses are able to maintain a healthy voltage profile across the network, and expect them not to act too often or change voltage magnitudes too drastically, which might otherwise degrade the performance of the frequency controller; in this regard, voltage magnitudes at the load buses are assumed to be constant, i.e., $V_l(t) = V_l$, $l \in \mathcal{V}_p^{(L)}$, for all t. Therefore, in the remainder, we only focus on the frequency regulation problem, and for brevity, we drop the V-argument from all the functions that depend on it. However, we show through numerical simulations that the proposed frequency controller can achieve its objectives if the voltage droop controllers are not too aggressive.

In the following, we also assume that after a change in load $P_j^{(L)}(t)$, $j \in \mathcal{V}_p^{(L)}$, the proposed controller is fast enough to restore the system frequency to its nominal value before another load change occurs, i.e., $P_j^{(L)}(t)$ is assumed to be a constant, $P_j^{(L)}$, when the controller is being executed.

Let $\omega_i(t) := \omega^* + \dot{\theta}_i(t)$ denote the local frequency at node i. Then, in order to achieve active power load sharing in microgrids with purely inductive electrical lines, $\omega_i(t)$ is typically regulated via a frequency-droop controller of the form (see, e.g., [5])

$$\omega_i(t) = \omega^* + D_i^{-1}(P_i^* - P_i(\theta(t))), \quad (5)$$

where $D_i > 0$ is referred to as the droop coefficient, P_i^* is the active power reference of inverter $i \in \mathcal{V}_p^{(I)}$. In the literature (see, e.g., [19], [20]), D_i is picked so that inverters share the active power demand of the loads according to their power ratings as follows:

$$\frac{P_i^*}{P_j^*} = \frac{D_i}{D_j} = \frac{\overline{P}_i}{\overline{P}_j},\ i, j \in \mathcal{V}_p^{(I)}, \quad (6)$$

where $\overline{P}_i$ is the power rating of inverter i. The droop coefficient D_i needs to be carefully selected to ensure stability, since if it is too small, the system might become unstable [21]. However, if it is too large, then, the convergence might become too slow to stabilize the frequency in the presence of a time-varying load [5]. Additionally, the operation of the controller in (5) will result in a steady-state deviation of the frequency with respect to the nominal value. To eliminate this frequency deviation, a secondary frequency controller would need to be implemented in a centralized or distributed fashion, both of which require communications.

Based on this idea of using the frequency at each inverter node as a control variable in achieving active power reference tracking, in Section III, we propose a frequency controller of the form

$$\dot{\theta}_i(t) = u_i(t), \quad i \in \mathcal{V}_p^{(I)}, \quad (7)$$

where $u_i(t)$ is adjusted via a feedback control to track a

desired injection value, P_i^*, while regulating $\omega_i(t)$ to ω^*, i.e., controller $u_i(t)$ combines the functionalities of the primary and secondary controllers without a separation of time-scales. [The objectives to be met by the controller are stated formally in Section II-C.]

Next, by defining $\gamma_{ij} \coloneqq V_i V_j B_{ij}$, $i \neq j$, $i, j \in \mathcal{V}_p$, and differentiating (4), we obtain

$$\begin{bmatrix} \dot{P}^{(I)}(t) \\ \mathbf{0}_{n-m} \end{bmatrix} = L^{(p)}(\theta(t))\dot{\theta}(t), \tag{8}$$

where $\mathbf{0}_{n-m}$ is a vector of $(n-m)$ zeros, $L^{(p)}(\theta(t)) = [\{L_{ij}^{(p)}(\theta(t))\}_{i,j\in\mathcal{V}_p}]$, with $L_{ij}^{(p)}(\theta(t)) = -\gamma_{ij}\cos(\theta_i(t) - \theta_j(t))$, $i \neq j$, $i, j \in \mathcal{V}_p$, and $L_{ii}^{(p)}(\theta(t)) = \sum_{l\neq i, l\in\mathcal{V}_p} \gamma_{il}\cos(\theta_i(t) - \theta_l(t))$. The matrix $L^{(p)}(\theta(t))$ can be partitioned as follows:

$$L^{(p)}(\theta(t)) = \begin{bmatrix} L_I^{(p)}(\theta(t)) & L_{IL}^{(p)}(\theta(t)) \\ L_{LI}^{(p)}(\theta(t)) & L_L^{(p)}(\theta(t)) \end{bmatrix}, \tag{9}$$

where $L_I^{(p)}(\theta(t)) \in \mathbb{R}^{|\mathcal{V}_p^{(I)}|\times|\mathcal{V}_p^{(I)}|}$ and $L_L^{(p)}(\theta(t)) \in \mathbb{R}^{|\mathcal{V}_p^{(L)}|\times|\mathcal{V}_p^{(L)}|}$. We can rewrite (8) to obtain

$$\dot{P}^{(I)}(t) = S(\theta(t))\dot{\theta}^{(I)}(t), \tag{10}$$

$$\dot{\theta}^{(L)}(t) = (L_L^{(p)}(\theta(t)))^{-1}L_{LI}^{(p)}(\theta(t))\dot{\theta}^{(I)}(t), \tag{11}$$

where $\theta^{(I)}(t) = [\theta_1(t), \ldots, \theta_m(t)]^{\mathrm{T}}$, $\theta^{(L)}(t) = [\theta_{m+1}(t), \ldots, \theta_n(t)]^{\mathrm{T}}$, and $S(\theta(t))$ denotes the Schur complement of $L^{(p)}(\theta(t))$, i.e., $S(\theta(t)) = L_I^{(p)}(\theta(t)) - L_{IL}^{(p)}(\theta(t))(L_L^{(p)}(\theta(t)))^{-1}L_{LI}^{(p)}(\theta(t))$, where $L_L^{(p)}(\theta(t))$ is invertible for all t since the controller we propose in Section III enforces the so-called phase-cohesiveness property, i.e., $|\theta_i(t) - \theta_j(t)| \leq \epsilon$, $\forall\{i, j\} \in \mathcal{E}_p$, and $\epsilon \in [0, \frac{\pi}{2})$ [12]. [In the remainder, by slightly abusing terminology, we say that $P(\theta(t))$ satisfies the phase-cohesiveness property and $\theta(t)$ is phase-cohesive if the phase-cohesiveness property is preserved at time t.] Then, by combining (7) and (10) – (11), the dynamics of the microgrid can be described as follows:

$$\dot{\theta}^{(I)}(t) = u(t), \tag{12}$$

$$\dot{\theta}^{(L)}(t) = (L_L^{(p)}(\theta(t)))^{-1}L_{LI}^{(p)}(\theta(t))u(t), \tag{13}$$

$$\dot{P}^{(I)}(t) = S(\theta(t))u(t), \tag{14}$$

where $u(t) = [u_1(t), \ldots, u_m(t)]^{\mathrm{T}}$.

Remark 1. The model in (12) – (14) is described by only ODEs as opposed to the original system model represented by DAEs in (2) – (3) and (7). Although analytical properties of DAEs are very different from those of ODEs, as shown in [22, Theorem 1], the solutions of these two different types of systems are identical for the same initial conditions and for all t as long as $L_L^{(p)}(\theta(t))$ is invertible for all t which is ensured by the proposed controller. ■

Note that if the phase-cohesiveness property is satisfied at time t, then, $L^{(p)}(\theta(t))$ is the weighted Laplacian of the graph $\mathcal{G}_p$, and $S(\theta(t))$ is positive semidefinite with a single zero eigenvalue, the corresponding eigenvector of which being the all-ones vector, $\mathbb{1}_{\mathrm{I}}$. Also, the second smallest eigenvalue of $S(\theta(t))$, denoted by $\lambda_2(S(\theta(t)))$, is positive.

C. Control Objectives

Suppose at time $t = t_c$ a substantial load change occurs, which results in (i) the local frequencies $\omega_i(t)$, $\forall i \in \mathcal{V}_p$, deviating from their nominal value, ω^*, and (ii) a mismatch between the active power injections at the inverter nodes and their references. Let $\Delta P_l^{(L)}(t_c)$ denote this load perturbation at node $l \in \mathcal{V}_p^{(L)}$ at $t = t_c$, i.e., $P_l^{(L)}(t_c) = P_l^{(L)}(t_c^-) + \Delta P_l^{(L)}(t_c)$; then, the main control objectives for the controller proposed for the system in (12) – (14) are:

- O1 to track some desired injections, P_i^*, $i \in \mathcal{V}_p^{(I)}$, which satisfy: (P1) $\sum_{i\in\mathcal{V}_p^{(I)}} P_i^* = \sum_{l\in\mathcal{V}_p^{(L)}} P_l^{(L)}(t_c)$, and (P2) ensure that the resultant equilibrium point is phase-cohesive; and
- O2 to eliminate the frequency deviation that results from the load change, i.e., $\dot{\theta}_i(t) \to 0$ as $t \to \infty$, $i \in \mathcal{V}_p$.

Remark 2. To cope with the errors in the computation of the total load demand or sudden load changes which are highly likely in a more practical scenario, one of the generators will absorb all uncertainties caused by inaccurate computation of the total load demand and any unmodelled losses in the system by fixing its frequency to the nominal value, i.e., this generator will essentially operate as a voltage source with fixed frequency, while other generators will track their corresponding active power references. To facilitate stability analysis, we assume that the computation of the total load demand is accurate and sudden load changes do not occur. However, in the numerical simulations in Section IV, we introduce an error in the computation of the total load demand, and let one of the generators operate as a voltage source with fixed frequency. ■

Objectives O1 and O2 are the standard objectives for primary and secondary frequency controllers, respectively. However, many secondary frequency controllers proposed in the literature (see, e.g., [3], [7], [19]) do not maintain desired load sharing while driving the system frequency to the nominal value. Also, the proportional load power sharing in (6), based on the inverter power ratings, does not necessarily result in phase-cohesive operation. By contrast, the controller to be introduced in the next section, does not use a separation of time-scales to attain objectives O1 and O2; and the reference assignment scheme for P_i^*, $i \in \mathcal{V}_p^{(I)}$, to be introduced later ensures that P2 holds.

III. Active Power Load Sharing Control

In this section, we first propose a control strategy to provide frequency regulation and to achieve the desired active power load sharing among the inverters. We show that this control ensures semi-global convergence of the active power injections to the reference and eliminates the frequency error.

A. Controller Operation Description

Let P_i^* denote the desired power injected by inverter i, and assume it satisfies P1 and P2 as stated in objective O1. Then,

if for the system in (12) – (14), we were to use a controller of the form

$$u(t) = -\alpha(P^{(I)}(t) - P^*), \tag{15}$$

where $P^* = [P_1^*, \dots, P_m^*]^{\mathrm{T}}$ and $\alpha > 0$, it might be the case that $P^{(I)}(t)$ may not converge to P^* as $t \to \infty$. In fact, the system might become unstable, since the phase-cohesiveness property might be violated at some time and, as a result, the matrix $S(\theta(t))$ might not be always positive-semidefinite with a single zero eigenvalue. However, we can enforce the phase-cohesiveness property at all times if we modify the controller in (15) by replacing P^* with a piecewise constant reference signal, $P^r(t) = [P_1^r(t), \dots, P_m^r(t)]^{\mathrm{T}}$, based on the following observation to be proved later: when, at some $t = \tau$, the reference $P^r(t)$ is fixed to some constant value, for $t \geq \tau$, within some $\delta > 0$ of the actual power injections at inverter nodes, i.e., $\|P^{(I)}(\tau) - P^r(\tau)\|_2 \leq \delta$, the controller

$$u(t) = -\alpha(P^{(I)}(t) - P^r(t)) \tag{16}$$

drives $P^{(I)}(t) - P^r(t) \to 0$ as $t \to \infty$, while maintaining the phase-cohesiveness property at all times. When $\|P^{(I)}(t) - P^r(t)\|_\infty$ becomes very small, we move the reference $P^r(t)$ closer to the desired injection value P^* along the line connecting initial active power injections $P(\theta(t_0))$ and the reference P^*, and apply control in (16). This slow readjustment of $P^r(t)$ continues until it reaches P^*. We show later that picking $P^r(t)$ that way allows us to maintain the phase-cohesiveness property for all time t.

More formally, define $P[t] := P(\theta(t))$, and $\Delta P^{(L)}(t) = [\Delta P_{m+1}^{(L)}(t), \dots, \Delta P_n^{(L)}(t)]^{\mathrm{T}}$. Note that $P^{(I)}(t_c) = P^{(I)}(t_c^-) + h(\theta^{(I)}(t_c^-), P^{(L)}(t_c^-) + \Delta P^{(L)}(t_c))$ for some continuous function $h : \mathbb{R}^m \times \mathbb{R}^{n-m} \to \mathbb{R}^m$, and $P[t_c] = \begin{bmatrix} P^{(I)}(t_c^-) + h(\theta^{(I)}(t_c^-), P^{(L)}(t_c^-) + \Delta P^{(L)}(t_c)) \\ -(P^{(L)}(t_c^-) + \Delta P^{(L)}(t_c)) \end{bmatrix}$. Then, we trigger the controller at $t = t_0 > t_c$ by assuming $P[t_0] = P[t_c]$ and by choosing the reference value, $P^r(t)$, for $t \geq t_0$, as follows:

$$P^r(t) = (1 - \lambda(t))P^{(I)}(t_0) + \lambda(t)P^*, \tag{17}$$

where $\lambda(t) = \lambda(t_0^-) + \Delta\lambda$, with

$$\Delta\lambda = \frac{\delta - \underline{\delta}\sqrt{m}}{\|P^* - P^{(I)}(t_0)\|_2}, \tag{18}$$

and $\lambda(t_0^-) = 0$. When for some $t = t_1$, $P^{(I)}(t_1^-)$ is such that $\|P^{(I)}(t_1^-) - P^r(t_1^-)\|_\infty \leq \underline{\delta}$, we again increase $\lambda(t)$ by $\Delta\lambda$:

$$\lambda(t) = \lambda(t_1^-) + \Delta\lambda, \quad t_1 \leq t,$$

and use the expression in (17) to update the reference value. By denoting t_k as the reference update time for which $t_k^- = \arg_{t > t_{k-1}} \|P^{(I)}(t) - P^r(t)\|_\infty \leq \underline{\delta}$, $P^r(t)$ can be expressed in a more general form as follows:

$$P^r(t) = (1 - \lambda(t))P^{(I)}(t_0) + \lambda(t)P^*, \quad t_k \leq t < t_{k+1}, \tag{19}$$

where

$$\lambda(t) = \lambda(t_k^-) + \Delta\lambda, \quad t_k \leq t < t_{k+1}. \tag{20}$$

In a more compact form, (19) – (20) can be rewritten as follows:

$$P^r(t) = P^r(t_k^-) + \Delta P^r, \quad t_k \leq t < t_{k+1}, \tag{21}$$

where $P^r(t_0^-) = P^{(I)}(t_c)$ and $\Delta P^r = (\delta - \underline{\delta}\sqrt{m})\frac{P^* - P^{(I)}(t_0)}{\|P^* - P^{(I)}(t_0)\|_2}$; thus, at each $t = t_k$, we move $P^r(t)$ closer to P^* along the line connecting $P^{(I)}(t_0)$ and P^*. [Note that if at some time t, $\|P^{(I)}(t) - P^*\| < \delta$, then, we set $\lambda(t)$ to 1 and $P^r(t)$ to P^*.]

B. Stability Analysis

First, we prove a lemma to show that in order to preserve the phase-cohesiveness property for all $t \geq t_0$, it is sufficient for $P(\theta(t))$ to satisfy the following synchronization condition for all $t \geq t_0$ [12]:

$$\|M^{\mathrm{T}} L^\dagger P(\theta(t))\|_\infty \leq \sin\epsilon, \tag{22}$$

where $L^\dagger$ is the pseudoinverse of $L = [L_{ij}]$, with $L_{ij} = -\gamma_{ij}$, $i \neq j$, $i, j \in \mathcal{V}_p$, and $L_{ii} = \sum_{l \neq i, l \in \mathcal{V}_p} \gamma_{il}$. Note that L, different from the Laplacian $L^{(p)}(\theta(t))$, is another weighted Laplacian of graph $\mathcal{G}_p$ with a weight γ_{ij} assigned to an edge $\{i, j\} \in \mathcal{E}_p$.

Lemma 1. Suppose $\theta(t_0)$ is phase-cohesive, and $P(\theta(t))$ satisfies the synchronization condition in (22) for all $t \geq t_0$. Then, $\theta(t)$ is phase-cohesive, unique and continuous for all $t \geq t_0$.

Proof. We prove by contradiction. Suppose that even though $P(\theta(t))$ satisfies the synchronization condition in (22) for all $t \geq t_0$, there is time $t = \tau > t_0$ at which $|\theta_i(\tau) - \theta_j(\tau)| = \frac{\pi}{4} + \frac{\epsilon}{2} > \epsilon$ for some $\{i, j\} \in \mathcal{E}_p$. However, since $\frac{\pi}{4} + \frac{\epsilon}{2} < \frac{\pi}{2}$, $L_L^{(p)}(\theta(t))$ is still invertible which implies that the solution of the system in (12) – (14) is continuous and unique over $t \in [t_0, \tau]$. Since $P(\theta(t))$ satisfies the synchronization condition in (22), there is corresponding $\theta \in \mathbb{R}^n$ which is phase-cohesive, i.e., $|\theta_i - \theta_j| \leq \epsilon$, $\forall\{i, j\} \in \mathcal{E}_p$, which contradicts the fact that there is only one θ for any given p such that $p = P(\theta)$ and $|\theta_i - \theta_j| < \frac{\pi}{2}$, $\forall\{i, j\} \in \mathcal{E}_p$ (see [23, Corollary 1]). □

Remark 3. The synchronization condition in (22) is both necessary and sufficient for the existence of a phase-cohesive solution in tree networks, and necessary and generically sufficient in cyclic networks except for some extreme cases when satisfaction of this condition does not guarantee the existence of a phase-cohesive solution. However, the authors of [12] numerically demonstrated that, for ten commonly studied IEEE test networks, this condition is sufficient. ■

Now, we state the main stability result.

Proposition 1. Consider the system in (12) – (14). Suppose that $\theta(t_0)$ is phase-cohesive and $P[t_0]$ and $\begin{bmatrix} P^* \\ -P^{(L)}(t_c) \end{bmatrix}$ satisfy a more strict version of the synchronization condition in (22), given by

$$\|M^{\mathrm{T}} L^\dagger P(\theta(t))\|_\infty \leq \kappa \sin\epsilon, \tag{23}$$

where

$$\kappa = \frac{1}{\sin\epsilon} \max\left\{ \|M^{\mathrm{T}} L^\dagger P[t_0]\|_\infty, \left\| M^{\mathrm{T}} L^\dagger \begin{bmatrix} P^* \\ -P^{(L)}(t_c) \end{bmatrix} \right\|_\infty \right\}. \tag{24}$$

Suppose that $\delta = \frac{1-\kappa}{\eta}\sin\epsilon$ with $\eta = \|M^{\mathrm{T}}X\|_\infty$, where X is a submatrix of $L^\dagger$ formed by its first m columns. Then, the controller in (16) with the reference in (21) ensures that the phase-cohesiveness property is maintained for all $t \geq t_0$, $P^{(I)}(t) \to P^*$ and $\theta(t) \to \theta^*$ as $t \to \infty$, where θ^* corresponds to P^*. ■

Before we prove our main result, we need the result in the following lemma.

Lemma 2. If $\|P^{(I)}(t_k^-) - P^r(t_k^-)\|_\infty \leq \underline{\delta}$, then, $\Delta\lambda$ in (18) guarantees that $\|P^{(I)}(t_k^-) - P^r(t_k)\|_2 \leq \delta$.

Now, we are ready to prove Proposition 1.

Proof. Define $\Delta P^{(I)}(t) = P^{(I)}(t) - P^r(t)$. Then, since $P[t_0]$ and $\begin{bmatrix} P^* \\ -P^{(L)}(t_c)\end{bmatrix}$ satisfy the synchronization condition in (23), and, for all $t \geq t_0$, $\lambda(t) \in [0,1]$, by using triangle inequality, we obtain that

$$\begin{aligned}
&\left\|M^{\mathrm{T}}L^\dagger \begin{bmatrix} P^r(t_0) \\ -P^{(L)}(t_c)\end{bmatrix}\right\|_\infty \\
&\leq \left\|M^{\mathrm{T}}L^\dagger \left((1-\lambda(t_0))P[t_0] + \lambda(t_0)\begin{bmatrix} P^* \\ -P^{(L)}(t_c)\end{bmatrix}\right)\right\|_\infty \\
&\leq (1-\lambda(t_0))\|M^{\mathrm{T}}L^\dagger P[t_0]\|_\infty \\
&+ \lambda(t_0)\left\|M^{\mathrm{T}}L^\dagger \begin{bmatrix} P^* \\ -P^{(L)}(t_c)\end{bmatrix}\right\|_\infty \leq \kappa\sin\epsilon,
\end{aligned}$$

which implies that any point on the line connecting $P[t_0]$ and $\begin{bmatrix} P^* \\ -P^{(L)}(t_c)\end{bmatrix}$ satisfies the synchronization condition given in (23). Let $\mathbb{1}_{\mathrm{L}}$ denote the all-ones vector of dimension $|\mathcal{V}_p^{(L)}|$. Then, since $\mathbb{1}_{\mathrm{I}}^{\mathrm{T}}P^{(I)}(t) = \mathbb{1}_{\mathrm{I}}^{\mathrm{T}}P^* = \mathbb{1}_{\mathrm{L}}^{\mathrm{T}}P^{(L)}(t_c)$, it follows that, for $t \in [t_0, t_1)$, we have that

$$\begin{aligned}
\mathbb{1}_{\mathrm{I}}^{\mathrm{T}}P^r(t) &= (1-\lambda(t))\mathbb{1}_{\mathrm{I}}^{\mathrm{T}}P^{(I)}(t_0) + \lambda(t)\mathbb{1}_{\mathrm{I}}^{\mathrm{T}}P^* \\
&= \mathbb{1}_{\mathrm{L}}^{\mathrm{T}}P^{(L)}(t_c),
\end{aligned}$$

therefore, $\mathbb{1}_{\mathrm{I}}^{\mathrm{T}}(P^{(I)}(t_0) - P^r(t_0)) = 0$. Since $\mathbb{1}_{\mathrm{I}}$ is an eigenvector of $S(\theta(t))$ corresponding to a single zero eigenvalue, then, by the Courant-Fischer Theorem [24, Theorem 4.2.6], we obtain that

$$\begin{aligned}
&(P^{(I)}(t_0) - P^r(t_0))^{\mathrm{T}}S(\theta(t_0))(P^{(I)}(t_0) - P^r(t_0)) \\
&\geq \lambda_2(S(\theta(t_0)))\|P^{(I)}(t_0) - P^r(t_0)\|_2^2. \qquad (25)
\end{aligned}$$

Since, by assumption, $\theta(t_0)$ satisfies the phase-cohesiveness property, $S(\theta(t_0))$ is positive-semidefinite, and $\lambda_2(S(\theta(t_0))) > 0$. Under the control in (16), the system in (14) can be written as follows:

$$\dot{P}^{(I)}(t) = -\alpha S(\theta(t))(P^{(I)}(t) - P^r(t)).$$

Then, for small positive $h < t_1 - t_0$, we use the Taylor series expansion to obtain $P^{(I)}(t_0 + h) = P^{(I)}(t_0) - h\alpha S(\theta(t_0))(P^{(I)}(t_0) - P^r(t_0)) + \mathcal{O}(h)$, arriving at (26) – (28), where, in the last inequality, we used (25). For small enough h, $2\alpha\lambda_2(S(\theta(t_0)))\|P^{(I)}(t_0) - P^r(t_0)\|_2^2$ dominates $\mathcal{O}(h)$; therefore, $\frac{1}{h}(\|\Delta P^{(I)}(t_0+h)\|_2^2 - \|\Delta P^{(I)}(t_0)\|_2^2) \leq 0$ and $\|\Delta P^{(I)}(t_0+h)\|_2 \leq \delta$ because $\|\Delta P^{(I)}(t_0)\|_2 \leq \delta$ by Lemma 2. Then, by using the triangle inequality and the submultiplicative property for matrix norms, we obtain that

$$\begin{aligned}
\|M^{\mathrm{T}}L^\dagger P[t_0+h]\|_\infty &\leq \left\|M^{\mathrm{T}}L^\dagger \begin{bmatrix} P^r(t_0+h) \\ -P^{(L)}(t_c)\end{bmatrix}\right\|_\infty \\
&+ \left\|M^{\mathrm{T}}L^\dagger \begin{bmatrix} \Delta P^{(I)}(t_0+h) \\ 0\end{bmatrix}\right\|_\infty \leq \kappa\sin\epsilon \\
&+ \|M^{\mathrm{T}}X\|_\infty\|\Delta P^{(I)}(t_0+h)\|_\infty \leq \kappa\sin\epsilon + \eta\delta,
\end{aligned}$$

where, in the last inequality, we used $\|\Delta P^{(I)}(t_0+h)\|_\infty \leq \|\Delta P^{(I)}(t_0+h)\|_2 \leq \delta$. By choosing $\delta = \frac{1-\kappa}{\eta}\sin\epsilon$, $\kappa\sin\epsilon + \eta\delta = \sin\epsilon$, therefore, $\|M^{\mathrm{T}}L^\dagger P[t_0+h]\|_\infty \leq \sin\epsilon$, and $P(t_0+h)$ satisfies the synchronization condition given in (22). Therefore, by Lemma 1, $\theta(t_0+h)$ is phase cohesive, which further implies that the matrix $S(\theta(t_0+h))$ is positive-semidefinite. Then, it follows that $S(\theta(t))$ is always positive-semidefinite and, therefore, $P^{(I)}(t) \to P^*$ as $t \to \infty$. Finally, it remains to show that $\theta(t) \to \theta^*$ as $t \to \infty$. By considering the following transformation: $x_i(t) = \theta_i(t) - \theta_1(t)$ and $x_i^* = \theta_i^* - \theta_1^*$, $1 \leq i \leq n$, and by using the Bolzano-Weierstrass Theorem and the uniqueness of the phase-cohesive θ^* corresponding to P^* it can be shown that $x(t) \to x^*$. Then, by considering $t \geq t_k$ when $P^r(t) = P^*$ and by using the fact that $\mathbb{1}_{\mathrm{I}}^{\mathrm{T}}\dot{\theta}^{(I)} = -\alpha\sum_{i\in\mathcal{V}^{(I)}}(P_i(t) - P_i^*) = 0$ and the uniqueness of the phase-cohesive θ^* corresponding to P^*, it can be shown that $\theta(t) \to \theta^*$. □

Here, we extend the result in Proposition 1 to the case when one of the inverters fixes its frequency.

Corollary 1. Consider the system in (12) – (14). Suppose that $\dot{\theta}_m(t) = 0$, for all t, $\theta(t_0)$ is phase-cohesive and $P[t_0]$ and $\begin{bmatrix} P^* \\ -P^{(L)}(t_c)\end{bmatrix}$ satisfy (23). Then, the controller

$$\begin{aligned}
\dot{\theta}_i &= -\alpha(P_i(t) - P_i^r(t)), \quad i = 1, \ldots, m-1, \\
P_i^r(t) &= P_i^r(t_k^-) + \Delta P_i^r, \quad t_k \leq t < t_{k+1}, \\
\Delta P_i^r &= (\delta - \underline{\delta}\sqrt{m})\frac{P_i^* - P_i^{(I)}(t_0)}{\left((m+1)\sum_{i=1}^{m-1}(P_i^* - P_i^{(I)}(t_0))^2\right)^{\frac{1}{2}}},
\end{aligned}$$

ensures that the phase-cohesiveness property is maintained for all $t \geq t_0$, $P^{(I)}(t) \to P^*$ and $\theta(t) \to \theta^*$ as $t \to \infty$. ■

Next, we provide an upper bound on the time it takes for the injections to converge to the desired injection value within a small error bound.

Lemma 3. Let $t = T$ denote the time it takes for $P^{(I)}(t)$ to converge to P^* within a small error bound, i.e., $\|P^{(I)}(t) - P^*\|_\infty \leq \underline{\delta}\sqrt{m}$. Assuming $t_k = \inf_t \arg_{t>t_{k-1}}\|P^{(I)}(t) - P^r(t)\|_\infty \leq \underline{\delta}$, we have that

$$T \leq \frac{\|P^* - P^{(I)}(t_0)\|_2 + \underline{\delta}\sqrt{m}}{\alpha\lambda_2(L)(\delta - \underline{\delta}\sqrt{m})\cos(\epsilon)}\ln\frac{\delta}{\underline{\delta}\sqrt{m}}. \qquad (29)$$

IV. Active Power Reference Assignment

In this section, we discuss how to choose the desired injections distributively for tree networks, as well as for networks

$$\frac{1}{h}(\|\Delta P^{(I)}(t_0+h)\|_2^2 - \|\Delta P^{(I)}(t_0)\|_2^2) = \frac{1}{h}(P^{(I)}(t_0+h) - P^{(I)}(t_0))^{\mathrm{T}}(P^{(I)}(t_0+h) + P^{(I)}(t_0) - 2P^r(t_0)) \tag{26}$$

$$= \frac{1}{h}(-h\alpha S(\theta(t_0))(P^{(I)}(t_0) - P^r(t_0)) + \mathcal{O}(h))^{\mathrm{T}}(2P^{(I)}(t_0) - h\alpha S(\theta(t_0))(P^{(I)}(t_0) - P^r(t_0)) + \mathcal{O}(h) - 2P^r(t_0)) \tag{27}$$

$$\leq -2\alpha\lambda_2(S(\theta(t_0)))\|P^{(I)}(t_0) - P^r(t_0)\|_2^2 + \mathcal{O}(h). \tag{28}$$

that have non-overlapping cycles (any pair of cycles does not share any common edge) so as the resulting equilibrium point satisfies the phase-cohesiveness property.

A. Tree Networks

Let $P_i^{(0)}$ denote the reference signal to inverter $i \in \mathcal{V}_p^{(I)}$ as determined by the load power sharing criterion in (6), i.e., $P_i^* = P_i^{(0)} := \frac{D_i}{\sum_{j\in\mathcal{V}_p^{(I)}} D_j}\sum_{l\in\mathcal{V}_p^{(L)}} P_l^{(L)}(t_c)$; next, we discuss an alternative to this reference choice. To this end, we formulate the following quadratic optimization problem:

$$\min_{p\in\mathbb{R}^n,\phi\in\mathbb{R}^{|\mathcal{E}|}} \ \|p - p^{(0)}\|_2^2 + \|\phi\|_2^2 \tag{30}$$

$$\text{subject to } p = M\Gamma\phi, \tag{31}$$

$$\underline{P}_i \leq p_i \leq \overline{P}_i, \quad \forall i \in \mathcal{V}_p, \tag{32}$$

$$-\kappa_0 \leq \phi_{ij} \leq \kappa_0, \quad \forall\{i,j\} \in \mathcal{E}_p, \tag{33}$$

which we refer to as QP1, where $\phi = [\{\phi_{ij}\}_{\{i,j\}\in\mathcal{E}_p}]^{\mathrm{T}}$, $\underline{P}_i = \overline{P}_i = -P_i^{(L)}$, $i \in \mathcal{V}_p^{(L)}$, the constraint (31) is a flow balance constraint that follows from (4), (32) and (33) are the box constraints on the power injections and normalized flows, constant parameter $\kappa_0 \in (0, \sin\epsilon)$, $p^{(0)} = [p_1^{(0)}, \ldots, p_n^{(0)}]^{\mathrm{T}}$ with $p_i^{(0)} = P_i^{(0)}$, $i \in \mathcal{V}_p^{(I)}$, and $p_i^{(0)} = -P_i^{(L)}$, $i \in \mathcal{V}_p^{(L)}$.

The solution of QP1, denoted by (p^*, ϕ^*), will be used to assign the desired injection P^*, i.e., $P^* = [p_1^*, \ldots, p_m^*]^{\mathrm{T}}$, for the controller in (16). By penalizing deviation of p from $p^{(0)}$ in the cost function of QP1 in (30), we aim to preserve the active power sharing among inverters according to their power ratings. The second term in the cost function allows us to minimize the flows along the electrical lines, which in general results in an increase of the step δ, and an improvement of the convergence rate of the controller in (16). Next, we show how to solve QP1 distributively.

First, we reformulate QP1 by introducing additional variables and constraints, the goal of which is to obtain an equivalent problem with a structure that is amenable to a solution via the alternating direction method of multipliers (ADMM) (see, e.g. [25, Section 3.4]). To this end, introduce variables $\phi_{ij}^{(i)}$ and $\phi_{ij}^{(j)}$, and define $x^{(i)} = \{\phi_{ij}^{(i)}\}_{\{i,j\}\in\mathcal{E}_p}$ and $z^{(i)} = \{\phi_{ji}^{(i)}\}_{\{i,j\}\in\mathcal{E}_p}$. Then, clearly, QP1 is equivalent to the following optimization problem:

$$\min_{p,x,z} \ \|p - p^{(0)}\|_2^2 + \|x\|_2^2$$

$$\text{subject to } \forall i \in \mathcal{V}_p, p_i = \sum_{j\in\mathcal{N}_i^+} \gamma_{ij}\phi_{ij}^{(i)} - \sum_{j\in\mathcal{N}_i^-} \gamma_{ij}\phi_{ji}^{(i)},$$

$$\underline{P}_i \leq p_i \leq \overline{P}_i,$$

$$\forall\{i,j\} \in \mathcal{E}_p, -\kappa_0 \leq \phi_{ij}^{(i)} \leq \kappa_0,$$

$$-\kappa_0 \leq \phi_{ij}^{(j)} \leq \kappa_0, \phi_{ij}^{(i)} = \phi_{ij}^{(j)},$$

which we refer to as QP2, where $x = [(x^{(1)})^{\mathrm{T}}, \ldots, (x^{(n)})^{\mathrm{T}}]^{\mathrm{T}}$, and $z = [(z^{(1)})^{\mathrm{T}}, \ldots, (z^{(n)})^{\mathrm{T}}]^{\mathrm{T}}$, $\mathcal{N}_i^+ = \{j : M_{je} = -1, e = \mathbb{I}(\{i,j\}), \{i,j\} \in \mathcal{E}_p\}$, $\mathcal{N}_i^- = \{j : M_{je} = 1, e = \mathbb{I}(\{i,j\}), \{i,j\} \in \mathcal{E}_p\}$. Then, the augmented Lagrangian for QP2 is given by

$$\begin{aligned} L_\rho(p,x,z,\mu,\nu) =& \|p - p^{(0)}\|_2^2 + \|x\|_2^2 \\ &+ \sum_{i=1}^m \mu_i(p_i - \sum_{j\in\mathcal{N}_i^+}\gamma_{ij}\phi_{ij}^{(i)} + \sum_{j\in\mathcal{N}_i^-}\gamma_{ij}\phi_{ji}^{(i)}) \\ &+ \sum_{i=1}^m \frac{\rho}{2}(p_i - \sum_{j\in\mathcal{N}_i^+}\gamma_{ij}\phi_{ij}^{(i)} + \sum_{j\in\mathcal{N}_i^-}\gamma_{ij}\phi_{ji}^{(i)})^2 \\ &+ \sum_{\{i,j\}\in\mathcal{E}_p}\Big(\nu_{ij}(\phi_{ij}^{(i)} - \phi_{ij}^{(j)}) + \frac{\rho}{2}(\phi_{ij}^{(i)} - \phi_{ij}^{(j)})^2\Big), \end{aligned}$$

where $\rho > 0$ is a constant parameter, $\mu \in \mathbb{R}^n$ and $\nu \in \mathbb{R}^{|\mathcal{E}|}$. To solve QP2, we apply ADMM, the iterations of which are given by

$$\begin{bmatrix} p[k+1] \\ x[k+1] \end{bmatrix} = \mathrm{argmin}_{(p,x)\in\mathcal{D}} L_\rho(p,x,z[k],\mu[k],\nu[k]), \tag{34}$$

$$z[k+1] = \mathrm{argmin}_{z\in\mathcal{D}'} L_\rho(p[k+1],x[k+1],z,\mu[k],\nu[k]), \tag{35}$$

$$\begin{aligned} \mu_i[k+1] =& \mu_i[k] + \rho(p_i[k+1] - \sum_{j\in\mathcal{N}_i^+}\gamma_{ij}\phi_{ij}^{(i)}[k+1] \\ &+ \sum_{j\in\mathcal{N}_i^-}\gamma_{ij}\phi_{ji}^{(i)}[k+1]), \end{aligned} \tag{36}$$

$$\nu_{ij}[k+1] = \nu_{ij}[k] + \rho(\phi_{ij}^{(i)}[k+1] - \phi_{ij}^{(j)}[k+1]), \tag{37}$$

for all $i \in \mathcal{V}_p$ and $\{i,j\} \in \mathcal{E}_p$, where $\mathcal{D} = \{(p,x) : \underline{P}_j \leq p_j \leq \overline{P}_j, \forall j \in \mathcal{V}_p, -\kappa_0 \leq \phi_{ij}^{(i)} \leq \kappa_0, \forall\{i,j\} \in \mathcal{E}_p\}$ and $\mathcal{D}' = \{z : -\kappa_0 \leq \phi_{ji}^{(i)} \leq \kappa_0, \forall(j,i) \in \mathcal{E}_p\}$.

The iterations in (34) – (35) can be written for each node i as follows:

$$\begin{aligned} &\begin{bmatrix} p_i[k+1] \\ x^{(i)}[k+1] \end{bmatrix} = \mathrm{argmin}_{(p_i,x^{(i)})\in\mathcal{D}_i}(p_i - p_i^{(0)})^2 + \|x^{(i)}\|_2^2 + \mu_i[k]p_i \\ &- \mu_i[k]\sum_{j\in\mathcal{N}_i^+}\gamma_{ij}\phi_{ij}^{(i)} + \frac{\rho}{2}(p_i - \sum_{j\in\mathcal{N}_i^+}\gamma_{ij}\phi_{ij}^{(i)} + \sum_{j\in\mathcal{N}_i^-}\gamma_{ij}\phi_{ji}^{(i)}[k])^2 \\ &+ \sum_{j\in\mathcal{N}_i^+}\Big(\nu_{ij}[k]\phi_{ij}^{(i)} + \frac{\rho}{2}(\phi_{ij}^{(i)} - \phi_{ij}^{(j)}[k])^2\Big), \end{aligned} \tag{38}$$

$$\begin{aligned} &z^{(i)}[k+1] = \mathrm{argmin}_{z^{(i)}\in\mathcal{D}_i'}\mu_i[k]\sum_{j\in\mathcal{N}_i^-}\gamma_{ij}\phi_{ji}^{(i)} - \sum_{j\in\mathcal{N}_i^-}\nu_{ji}[k]\phi_{ji}^{(i)} \\ &+ \frac{\rho}{2}(p_i[k+1] - \sum_{j\in\mathcal{N}_i^+}\gamma_{ij}\phi_{ij}^{(i)}[k+1] + \sum_{j\in\mathcal{N}_i^-}\gamma_{ij}\phi_{ji}^{(i)})^2 \\ &+ \sum_{j\in\mathcal{N}_i^-}\frac{\rho}{2}(\phi_{ji}^{(j)}[k+1] - \phi_{ji}^{(i)})^2, \end{aligned} \tag{39}$$

where $\mathcal{D}_i = \{(p_i, x^{(i)}) : \underline{P}_i \leq p_i \leq \overline{P}_i, -\kappa_0 \leq \phi_{ij}^{(i)} \leq \kappa_0, \forall j \in \mathcal{N}_i^+\}$ and $\mathcal{D}_i' = \{z^{(i)} : -\kappa_0 \leq \phi_{ji}^{(i)} \leq \kappa_0, \forall j \in \mathcal{N}_i^-\}$.

As shown in (38) – (39), in order to update $p_i[k]$, $x_i[k]$, and $z_i[k]$, each node i needs to solve two small box-constrained quadratic problems. They can be solved by using one of the interior-point methods (see, e.g., [26]). Alternatively, each box-constrained quadratic problem can be transformed to a least distance problem that can be solved by using [27, Theorem 5.2.1], which establishes the equivalence between a least distance problem and a nonnegative least squares problem, and an algorithm for solving a nonnegative least squares problem given in [28, Chapter 23]; the solution is guaranteed to be obtained after a finite number of iterations that typically depends linearly on the number of variables which is roughly the degree of a node i, $i \in \mathcal{V}_p$. The iterations in (36) – (39) can be executed in a distributive fashion whereby each node i only needs to obtain $\phi_{ji}^{(j)}[k+1]$ from every $j \in \mathcal{N}_i^-$, and $\phi_{ij}^{(j)}[k+1]$ from every $j \in \mathcal{N}_i^+$ by communicating with its neighbors.

If QP1 is feasible, then, by [29, Theorem 1], (34) – (37) converge to the optimal phase-cohesive solution $(p^*, \phi^*, \phi^*, \mu^*, \nu^*)$. However, solving QP1 does not necessarily yield a phase-cohesive solution if there are cycles in the network. Next, we show how to deal with the case when the network has non-overlapping cycles. To this end, we add an additional constraint to QP1 which guarantees phase-cohesiveness for the cyclic networks.

B. Networks with Non-Overlapping Cycles

Consider a network with c non-overlapping cycles, $\mathcal{C}_1, \ldots, \mathcal{C}_c$. Define $N = [n^{(1)}, \ldots, n^{(c)}]$, where $n^{(i)}$ satisfies $Mn^{(i)} = 0$ and corresponds to cycle $\mathcal{C}_i$ so that when $k = \mathbb{I}(\{l,j\})$, $n_k^{(i)} = 1$, if $\{l,j\} \in \mathcal{C}_i$, $n_k^{(i)} = -1$, if $\{j,l\} \in \mathcal{C}_i$, and 0, otherwise. Then, for a given set of injections p, any solution of (4) can be generally written as follows [12]:

$$\phi' = \phi + \Gamma^{-1} N \mu, \tag{40}$$

where ϕ is any particular solution to $p = M\Gamma\phi$, and $\mu \in \mathbb{R}^c$. Then, assuming $\phi_{ij} = -\phi_{ji}$, $\forall \{i,j\} \in \mathcal{E}_p$, define $\overline{\mu}_i(\phi) = \min_{\{l,j\} \in \mathcal{C}_i} \gamma_{lj}(\kappa_0 - \phi_{lj})$, $\underline{\mu}_i(\phi) = \max_{\{l,j\} \in \mathcal{C}_i} \gamma_{lj}(-\kappa_0 - \phi_{lj})$ and $g_i(\phi) = \sum_{\{l,j\} \in \mathcal{C}_i} \arcsin(\phi_{lj})$. By using the single cycle feasibility lemma in [12], the following result becomes obvious.

Lemma 4. Suppose $p = M\Gamma\phi$, $-\kappa_0 \le \phi_{ij} \le \kappa_0$, $\forall \{i,j\} \in \mathcal{E}_p$, $\underline{P}_i \le p_i \le \overline{P}_i$, $\forall i \in \mathcal{V}_p^{(I)}$, $p_i = -P_i^{(L)}$, $\forall i \in \mathcal{V}_p^{(L)}$. Then, p satisfies the phase-cohesiveness property for a network with non-overlapping cycles, $\mathcal{C}_1, \ldots, \mathcal{C}_c$, if $g_i(\phi + \Gamma^{-1} n^{(i)} \overline{\mu}_i(\phi)) \ge 0$ and $g_i(\phi + \Gamma^{-1} n^{(i)} \underline{\mu}_i(\phi)) \le 0$ for $i = 1, 2, \ldots, c$. □

For some $\beta \ge 0$, define $\mathcal{F}_i(\beta) = \{\phi : g_i(\phi + \Gamma^{-1} n^{(i)} \overline{\mu}_i(\phi)) \ge 0,\ g_i(\phi + \Gamma^{-1} n^{(i)} \underline{\mu}_i(\phi)) \le 0,\ \overline{\mu}_i(\phi) \ge \beta,\ \underline{\mu}_i(\phi) \le -\beta\}$. Now, we state the following lemma:

Lemma 5. Suppose d_i is the number of edges in cycle $\mathcal{C}_i$, $\overline{\gamma}_i = \max_{\{l,j\} \in \mathcal{C}_i} \gamma_{lj}\kappa_0$, $\underline{\gamma}_i = \min_{\{l,j\} \in \mathcal{C}_i} \gamma_{lj}\kappa_0$, $\epsilon_0 = \arcsin(\kappa_0)$, and $\psi_i = \frac{\epsilon_0}{d_i - 1}$. If

$$\beta_i^* = \frac{1}{2}\overline{\gamma}_i - \frac{\underline{\gamma}_i}{2}\sin(\psi_i), \tag{41}$$

then, $\mathcal{F}_i(\beta_i^*)$ is convex and $\mathcal{F}_i(\beta_i^*) \equiv \mathcal{B}_i$, where $\mathcal{B}_i \coloneqq \{\phi : -\kappa_0 + \frac{\beta_i^*}{\gamma_{lj}} \le \phi_{lj} \le \kappa_0 - \frac{\beta_i^*}{\gamma_{lj}}, \forall \{l,j\} \in \mathcal{C}_i\}$.

Proof. Define $\mathcal{M}_i = \{\phi : \overline{\mu}_i(\phi) \ge \beta_i^*, \underline{\mu}_i(\phi) \le -\beta_i^*\}$. We show that $\mathcal{B}_i \equiv \mathcal{M}_i$. Suppose that $\phi \in \mathcal{B}_i$. Since $\phi_{lj} \le \kappa_0 - \frac{\beta_i^*}{\gamma_{lj}}$, $\forall \{l,j\} \in \mathcal{C}_i$, and, by definition, $\overline{\mu}_i(\phi) = \min_{\{l,j\} \in \mathcal{C}_i} \gamma_{lj}(\kappa_0 - \phi_{lj})$, it follows that $\overline{\mu}_i(\phi) \ge \beta_i^*$. Similarly, $\underline{\mu}_i(\phi) \le -\beta_i^*$. Conversely, if $\phi \in \mathcal{M}_i$, then, $\overline{\mu}_i(\phi) = \min_{\{l,j\} \in \mathcal{C}_i} \gamma_{lj}(\kappa_0 - \phi_{lj}) \ge \beta_i^*$, and $\phi_{lj} \le \kappa_0 - \frac{\beta_i^*}{\gamma_{lj}}$. Similarly, if $\underline{\mu}_i(\phi) \le -\beta_i^*$, then, $-\kappa_0 + \frac{\beta_i^*}{\gamma_{lj}} \le \phi_{lj}$. Therefore, $\mathcal{B}_i \equiv \mathcal{M}_i$.

Now, we show that $\mathcal{F}_i(\beta_i^*) \equiv \mathcal{B}_i$. Because $\mathcal{F}_i(\beta_i^*) \subseteq \mathcal{M}_i$, then, it is enough to prove that, $\forall \phi \in \mathcal{M}_i$, $g_i(\phi + \Gamma^{-1} n^{(i)} \overline{\mu}_i(\phi)) \ge 0$, and $g_i(\phi + \Gamma^{-1} n^{(i)} \underline{\mu}_i(\phi)) \le 0$. Suppose $\phi \in \mathcal{M}_i$, then, by using (41) and the fact that $\mathcal{B}_i \equiv \mathcal{M}_i$, we have that, for $\{l,j\} \in \mathcal{C}_i$,

$$\begin{aligned}\phi_{lj} + \frac{\overline{\mu}_i(\phi)}{\gamma_{lj}} \ge & -\kappa_0 + \frac{2\beta_i^*}{\gamma_{lj}} = -\kappa_0 + \frac{\overline{\gamma}_i}{\gamma_{lj}} \\ & - \frac{\underline{\gamma}_i}{\gamma_{lj}}\sin(\psi_i) \ge -\sin(\psi_i).\end{aligned} \tag{42}$$

Define $\{a,b\} = \operatorname{argmin}_{\{l,j\} \in \mathcal{C}_i} \gamma_{lj}(\kappa_0 - \phi_{lj})$ and $\mathcal{C}_i' = \mathcal{C}_i \setminus \{a,b\}$. Then,

$$g_i(\phi + \Gamma^{-1} n^{(i)} \overline{\mu}_i(\phi)) = \epsilon_0 + \sum_{\{l,j\} \in \mathcal{C}_i'} \arcsin\left(\phi_{lj} + \frac{\overline{\mu}_i(\phi)}{\gamma_{lj}}\right).$$

By using (42) and the fact that $\arcsin(\cdot)$ is monotonically increasing, we obtain that

$$g_i(\phi + \Gamma^{-1} n^{(i)} \overline{\mu}_i(\phi)) \ge \epsilon_0 - \sum_{\{l,j\} \in \mathcal{C}_i'} \arcsin(\sin(\psi_i)) = 0.$$

Similary, $g_i(\phi + \Gamma^{-1} n^{(i)} \underline{\mu}_i(\phi)) \le 0$. Therefore, $\mathcal{F}_i(\beta_i^*) \equiv \mathcal{B}_i$, which is convex. □

Suppose for all i we have that $\mathcal{F}_i(\beta_i^*)$ is convex for some β_i^*. Then, the following quadratic optimization problem, which we refer to as QP3, can be used to find a phase-cohesive solution when there are non-overlapping cycles in the network:

$$\begin{aligned}\min_{p,x,z}\ & \|p - p^{(0)}\|_2^2 + \|x\|_2^2 \\ \text{subject to } \forall i \in \mathcal{V}_p, p_i = & \sum_{j \in \mathcal{N}_i^+} \gamma_{ij}\phi_{ij}^{(i)} - \sum_{j \in \mathcal{N}_i^-} \gamma_{ij}\phi_{ji}^{(i)}, \\ & \underline{P}_i \le p_i \le \overline{P}_i, \\ & \forall \{i,j\} \in \mathcal{E}_p, -\kappa_0 \le \phi_{ij}^{(i)} \le \kappa_0, \\ & -\kappa_0 \le \phi_{ij}^{(j)} \le \kappa_0, \\ & \phi_{ij}^{(i)} = \phi_{ij}^{(j)}, \\ & x, z \in \mathcal{F}_k(\beta_k^*), \forall k.\end{aligned}$$

Define $\mathcal{H}_i = \{(p_i, x^{(i)}) : \underline{P}_i \le p_i \le \overline{P}_i, -\kappa_0 \le \phi_{ij}^{(i)} \le \kappa_0, \forall j \in \mathcal{N}_i^+, x^{(i)} \in \mathcal{F}_k(\beta_k^*), \forall k\}$ and $\mathcal{H}_i' = \{z^{(i)} : -\kappa_0 \le \phi_{ji}^{(i)} \le \kappa_0, \forall j \in \mathcal{N}_i^-, z^{(i)} \in \mathcal{F}_k(\beta_k^*), \forall k\}$. The ADMM iterations for QP3 are the same as in (36) – (39) except that instead of the sets $\mathcal{D}_i$ and $\mathcal{D}_i'$, $\mathcal{H}_i$ and $\mathcal{H}_i'$ are used as constraint sets for $(p_i, x^{(i)}, z^{(i)})$. Projection onto the sets $\mathcal{H}_i$ and $\mathcal{H}_i'$ can be difficult to compute. However, if we choose β_k^* as

in (41), $\forall k$, then, $\mathcal{H}_i$ and $\mathcal{H}_i'$ simplify to $\mathcal{H}_i = \{(p_i, x^{(i)}) : \underline{P}_i \leq p_i \leq \overline{P}_i, -\kappa_0 \leq \phi_{ij}^{(i)} \leq \kappa_0, \forall j \in \mathcal{N}_i^+, -\kappa_0 + \frac{\beta_k^*}{\gamma_{ij}} \leq \phi_{ij}^{(i)} \leq \kappa_0 - \frac{\beta_k^*}{\gamma_{ij}}, \text{if } \{i,j\} \text{ or } \{j,i\} \in \mathcal{C}_k, \forall k\}$, and $\mathcal{H}_i' = \{z^{(i)} : -\kappa_0 \leq \phi_{ji}^{(i)} \leq \kappa_0, \forall j \in \mathcal{N}_i^-, -\kappa_0 + \frac{\beta_k^*}{\gamma_{ij}} \leq \phi_{ji}^{(i)} \leq \kappa_0 - \frac{\beta_k^*}{\gamma_{ij}}, \text{if } \{j,i\} \text{ or } \{i,j\} \in \mathcal{C}_k, \forall k\}$.

V. Distributed Implementation

Recall the controller proposed in Section III for the system in (12) – (14):

$$u(t) = -\alpha(P^{(I)}(t) - P^r(t)) \tag{43}$$

where

$$P^r(t) = P^r(t_k^-) + \Delta P^r, \quad t_k \leq t < t_{k+1}, \tag{44}$$

and $\Delta P^r = (\delta - \underline{\delta}\sqrt{m})\frac{P^* - P^{(I)}(t_0)}{\|P^* - P^{(I)}(t_0)\|_2}$. In order to execute (43) – (44), it is necessary to compute P^*, δ, and $\|P^* - P^{(I)}(t_0)\|_2$, for which global information is required. In this section, we show how to compute these quantities distributively; to this end, we rely on consensus-type algorithms, the basics of which are reviewed next.

A. Distributed Algorithms

To enable a distributed implementation of the controller in (43) – (44), we require each node of the physical layer to have bidirectional communication links with all its neighbor nodes. Let $\mathcal{G}_c = (\mathcal{V}_c, \mathcal{E}_c)$ denote the graph describing the exchange of information among local processors located at the nodes of the physical network; then, $\mathcal{V}_c = \mathcal{V}_p$, and $\mathcal{E}_c = \mathcal{E}_p$; and the weighted Laplacian for $\mathcal{G}_c$ can be chosen the same as that of $\mathcal{G}_p$, i.e., L used earlier in (22). Next, we describe several well-established iterative algorithms that can be executed over $\mathcal{G}_c$, and that serve as primitives to distributively compute the quantities of interest, i.e., P^*, δ, and $\|P^* - P^{(I)}(t_0)\|_2$.

1) Average Consensus: Consider the vector $v = [v_1, \ldots, v_n]^{\mathrm{T}}$, where v_i is known only to node i. Suppose every node requires to know $\sum_{i \in \mathcal{V}_p} v_i$. Then, consider the following discrete-time average consensus protocol:

$$\overline{x}[k+1] = A\overline{x}[k], \tag{45}$$

where $A = I - \chi L$ with positive constant $\chi < \frac{1}{\max_{i \in \mathcal{V}_p} L_{ii}}$, $\overline{x}[k] = [\overline{x}_1[k], \ldots, \overline{x}_n[k]]^{\mathrm{T}}$ with $\overline{x}_i[k]$ being updated at node i. If each node i initializes $\overline{x}_i[0] = v_i$, then, $\overline{x}_i[k] \to \frac{1}{n}\sum_{j \in \mathcal{V}_p} \overline{x}[0] = \frac{1}{n}\sum_{j \in \mathcal{V}_p} v_i$ as $k \to \infty$ for sufficiently small χ (see, e.g., [30]).

For our application, we would like each node to terminate the protocol after a finite number of iterations, e.g., when $\overline{x}_i[k]$ is within some pre-specified value from $\frac{1}{n}\sum_{j \in \mathcal{V}_p} \overline{x}[0]$. This can be done by using the distributed stopping protocol proposed in [30], which determines distributively when to terminate the average consensus protocol in (45) once convergence is within acceptable tolerance.

2) Max-Consensus: Suppose every node requires to know $\|v\|_\infty = \max_{i \in \mathcal{V}_p} v_i$. Let $\mu_i[k]$ be an estimate for $\|v\|_\infty$ maintained by node $i \in \mathcal{V}_p$ at iteration k. Let $\mathcal{N}_i$ denote the set of neighbors of $i \in \mathcal{V}_p$; then, as shown in [30], if each node i initializes $\mu_i[0] = v_i$ and update its estimate according to

$$\mu_i[k+1] = \max_{j \in \mathcal{N}_i \cup \{i\}} \mu_j[k], \tag{46}$$

it follows that, after a finite number of iterations bounded from above by the diameter of the graph, every node can obtain $\|v\|_\infty$.

B. Reference Computation

To compute P^* using ADMM iterations in (36) – (39), we need to determine $P^{(0)} = [P_1^{(0)}, \ldots, P_m^{(0)}]^{\mathrm{T}}$, where $P_i^{(0)} = \frac{D_i}{\sum_{j \in \mathcal{V}_p^{(I)}} D_j} \sum_{l \in \mathcal{V}_p^{(L)}} P_l^{(L)}(t_c)$. We can compute $\sum_{j \in \mathcal{V}_p^{(I)}} D_j$, at the start-up of the system, and the total active power load demand, $\sum_{l \in \mathcal{V}_p^{(L)}} P_l^{(L)}(t_c)$, distributively by using the average consensus protocol in (45). To compute $\sum_{j \in \mathcal{V}_p^{(I)}} D_j$, each node i initializes $\overline{x}_i[0]$ as follows:

$$\overline{x}_i[0] = \begin{cases} D_i, & i \in \mathcal{V}_p^{(I)} \\ 0, & i \in \mathcal{V}_p^{(L)}. \end{cases} \tag{47}$$

Then, $\overline{x}_i[k] \to \frac{1}{n}\sum_{j \in \mathcal{V}_p^{(I)}} D_j$ as $k \to \infty$. Similarly, to compute $\sum_{l \in \mathcal{V}_p^{(L)}} P_l^{(L)}(t_c)$,

$$\overline{x}_i[0] = \begin{cases} 0, & i \in \mathcal{V}_p^{(I)} \\ P_i^{(L)}, & i \in \mathcal{V}_p^{(L)}, \end{cases} \tag{48}$$

which results in $\overline{x}_i[k] \to \frac{1}{n}\sum_{l \in \mathcal{V}_p^{(L)}} P_l^{(L)}(t_c)$ as $k \to \infty$.

C. Reference Step Computation

To find the reference step ΔP^r, we need to compute $\|P^* - P^{(I)}(t_0)\|_2$ and δ, which depends on ϵ, η, and κ. To compute $\|P^* - P^{(I)}(t_0)\|_2$, we use the average consensus protocol in (45), in which each node i initializes $\overline{x}_i[0]$ as follows:

$$\overline{x}_i[0] = \begin{cases} (P_i^* - P_i[t_0])^2, & i \in \mathcal{V}_p^{(I)} \\ 0, & i \in \mathcal{V}_p^{(L)}. \end{cases} \tag{49}$$

Then, $\overline{x}_i[k] \to \frac{1}{n}\|P^* - P^{(I)}(t_0)\|_2^2$ as $k \to \infty$. Next, we discuss how to find δ. At the start-up of the system, all nodes need to pick $\epsilon \in (0, \frac{\pi}{2})$ close to $\frac{\pi}{2}$ for larger δ. We use the following lemma (given without proof due to space limitation) to find an upper bound for $\eta = \|M^{\mathrm{T}} X\|_\infty$.

Lemma 6. Let m denote the number of inverters. Let R_{ij} denote the effective resistance between nodes i and $j \in \mathcal{V}_p$. Then,

$$\eta \leq \max_{\{i,j\} \in \mathcal{E}_p} \frac{3m}{2R_{ij}}. \tag{50}$$

By using Lemma 6, we compute an upper bound for η by running the max-consensus protocol in (46) at the start-up of the system, before we execute the controller. To find κ as defined in (24), we need to compute $\|M^{\mathrm{T}} L^\dagger P[t_0]\|_\infty$ and $\left\| M^{\mathrm{T}} L^\dagger \begin{bmatrix} P^* \\ -P^{(L)}(t_c) \end{bmatrix} \right\|_\infty$; next, we discuss how to compute the former as the computation of the latter quantity is similar. Define $y = L^\dagger P[t_0]$, then, we have that

$$P[t_0] = Ly. \tag{51}$$

If $\hat{y}$ is a particular solution to (51), then, $y^{(c)} = \hat{y} + c\mathbf{1}$, where c is any constant, is its general solution. Since $M^{\mathrm{T}} y^{(c)} = M^{\mathrm{T}} \hat{y}$, $\|M^{\mathrm{T}} L^{\dagger} P[t_0]\|_\infty = \|M^{\mathrm{T}} y^{(c)}\|_\infty$. We can obtain the general solution $y^{(c)}$ distributively by running a slight variation of the average consensus protocol in (45) as follows:

$$w[k+1] = \hat{y} + A(w[k] - \hat{y}), \tag{52}$$

where $w[k] = [w_1[k], \ldots, w_n[k]]^{\mathrm{T}}$ with $w[0]$ being all-zeros vector and $w_i[k]$ being updated at node i, which guarantees that $w[k] \to y^{(c)}$ as $k \to \infty$ [30]. However, $\hat{y}$ is unknown, which makes it impossible to implement the protocol in (52). However, since $L\hat{y} = P[t_0]$ is known, we can rewrite (52) as follows:

$$w[k+1] = Aw[k] + \chi P[t_0], \tag{53}$$

which can be implemented together with the distributed stopping protocol in [30]. Once we obtain $y^{(c)}$, we run the max-consensus protocol to compute $\|M^{\mathrm{T}} y^{(c)}\|_\infty$.

Finally, the max-consensus protocol is used to check if $P^{(I)}(t_k)$ is close to the reference $P^r(t_k)$, i.e., $\|P^{(I)}(t_k) - P^r(t_k)\|_\infty \leq \underline{\delta}$, so as to readjust $P^r(t_k)$ closer to P^* by using the step ΔP^r.

D. Timeline

We discuss how to carry out the initial execution of the frequency controller before all computations are completed. We assume that if a load change occurs at $t = t_c$, then, the total load change $\sum_{l \in \mathcal{V}_p^{(L)}} \Delta P_l^{(L)}(t_c)$ is available at $t = t_l > t_c$ and the new reference P^* and the reference step ΔP^r are available at $t = t_0 > t_l$. Define $\zeta_i(t) = \frac{P_i^*(t)}{\sum_{l \in \mathcal{V}_p^{(L)}} P_l^{(L)}(t)}$; then, for $t \in [t_c, t_l)$, we execute the conventional primary droop controller in (5) with droop coefficients $D_i = \chi \zeta_i(t_c^-)$, where χ is some positive constant. For $t \in [t_l, t_0^-]$, we execute the controller in (16) based on the following desired injection:

$$P_i^* = \zeta_i(t_c^-) \sum_{l \in \mathcal{V}^{(L)}} P_l^{(L)}(t_c), \quad t_l \leq t \leq t_0^-, \tag{54}$$

and the reference step ΔP^r corresponding to the pre-change load, $P^{(L)}(t_c^-)$. Note that if $P^{(I)}(t)$ does not converge to the P^* in (54) before $t = t_0$, at this instant we update the reference P^* and the reference step ΔP^r to the new values corresponding to $P^{(L)}(t_c)$. An overview of the order in which each value is computed is illustrated by the timeline in Fig. 1.

Remark 4. The above frequency regulation scheme for $t \in [t_c, t_0^-]$ aims to preserve the same load sharing as the one from the previous load perturbation. We assume that $\zeta_i(t)$ does not change significantly with time, since, typically, $|\mathbb{1}_{\mathrm{L}}^{\mathrm{T}} \Delta P^{(L)}(t_c)| \ll \mathbb{1}_{\mathrm{L}}^{\mathrm{T}} P^{(L)}(t_c)$, and $|\Delta P_l^{(L)}(t_c)| \ll P_l^{(L)}(t_c)$, $l \in \mathcal{V}_p^{(L)}$. ■

VI. Numerical Example

In this section, we illustrate the performance of the proposed controller for a 9-bus microgrid, the topology of which is shown in Fig. 2a. Nodes G_1, G_2, and G_3 correspond to inverters, with the remaining nodes corresponding to loads. Although in the stability analysis we assume constant voltage magnitudes, in this numerical example we demonstrate that the proposed controller has some robustness against voltage changes introduced by the standard voltage droop controller given by

$$V_i(t) = V_i^0 + m_i^{-1}(Q_i^*(t) - Q_i(t)), \quad i \in \mathcal{V}^{(I)}, \tag{55}$$

where V_i^0 is the nominal voltage, $m_i > 0$ is the voltage droop coefficient of inverter $i \in \mathcal{V}^{(I)}$, $Q_i^*(t)$ is the reactive power reference, and $Q_i(t)$ is the reactive power injection into the network via node $i \in \mathcal{V}^{(I)}$ given by

$$Q_i(t) = -\sum_{j \in \mathcal{V}} V_i(t) V_j(t) B_{ij} \cos(\theta_i(t) - \theta_j(t)), \tag{56}$$

where $B_{ii} = -\sum_{j \in \mathcal{V}} B_{ij}$. We also consider a more practical scenario when the electrical lines have unmodelled losses and the computation of the total load demand is not exact. In our simulations, the resistance-to-inductance ratio varies in the range $[0.05, 0.1]$ across the electrical lines, and the total load demand is computed with an error percentage in the range $[3, 7]$ %. Maximum allowable frequency deviation $\frac{\Delta\omega_{max}}{2\pi}$ was chosen to be 1.5 Hz.

To deal with losses and uncertainties, one of the generators provides for the unmodelled system losses and uncertainties due to the erroneous total active power demand computation by fixing its frequency to the nominal value; other generators track their corresponding active power references. Figure 2 shows the performance of the proposed control strategy for large load perturbations at $t = 0.6$ s, 4.6 s and 8.6 s. After each load perturbation, we are able to achieve the desired active power load sharing and regulate the frequency $\frac{\omega_i}{2\pi}$ at each inverter to the desired frequency value of 60 Hz. In order not to violate the maximum allowable frequency deviation, the upper bound on the feedback gain α was calculated as follows:

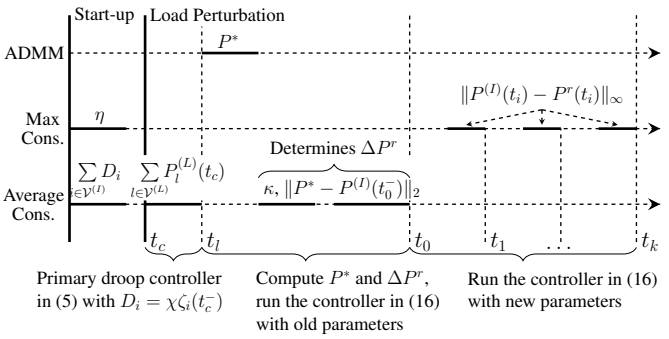

Fig. 1: Timeline of the execution of the proposed frequency controller and the computations involved in its distributed implementation.

TABLE I: Comparison between P^* and $P^{(0)}$ after a load change at $t = 0.6$ s.

	$\|\epsilon\|$	$\|\phi\|$	κ	δ	$\Delta\lambda$
P^*	$\frac{\pi}{2} - 0.01$	1.8388	0.7782	0.0278	0.2623
$P^{(0)}$	$\frac{\pi}{2} - 0.01$	2.3308	0.8090	0.0239	0.2410

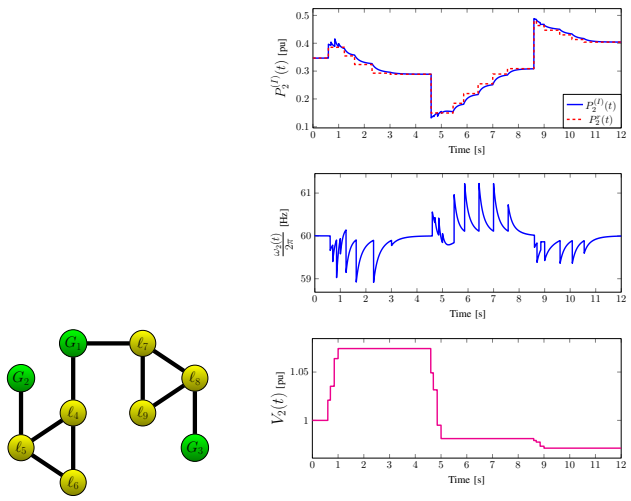

(a) (b)

Fig. 2: (a) 9-bus microgrid topology, (b) evolution of $P_2^{(I)}(t)$, $\frac{\omega_2(t)}{2\pi}$, and $V_2(t)$.

$\alpha \leq \frac{\Delta\omega_{max}}{\delta} = \frac{2\pi}{\delta}$. The ADMM iterations in (36) – (39) (with the cyclic constraint sets $\mathcal{H}_i$ and $\mathcal{H}_i'$ being used instead of $\mathcal{D}_i$ and $\mathcal{D}_i'$) were used to compute the reference P^* after each load perturbation.

Controller parameters are given in Table I. Since $\kappa < 1$ throughout the whole operation of the controller, P^* was always feasible by the synchronization condition given in (23). We also chose $\underline{\delta} = 0.005$ such that $\underline{\delta}\sqrt{m} < \delta$ for $m = 3$. Because QP3-based reference P^* minimizes the flows, the normalized flow ϕ and κ are typically smaller for P^* than for $P^{(0)}$ as also shown in Table I, which further gives larger δ and $\Delta\lambda$ and improves the convergence rate. As implied by (29), it is desirable to have larger $\Delta\lambda$ and smaller κ in order to increase the convergence rate. The convergence speed can also be improved if we increase $\underline{\delta}$, while satisfying $\underline{\delta}\sqrt{m} < \delta$, as established in (29) and confirmed by the numerical simulations.

VII. Concluding Remarks

We presented a control strategy which allows inverter-interfaced generators in a microgrid to track the desired injections semi-globally, and to restore the frequency to its nominal value by ensuring that the phase-cohesiveness property is always maintained. We computed the desired injections distributively by solving a quadratic optimization problem. This reference typically allows to have faster convergence rate than the one based on the power ratings of the inverters. We also showed how to compute the controller parameters distributively.

References

[1] D. Olivares *et al.*, "Trends in microgrid control," *IEEE Trans. Smart Grid*, vol. 5, no. 4, pp. 1905–1919, 2014.

[2] T. Vandoorn *et al.*, "Microgrids: Hierarchical control and an overview of the control and reserve management strategies," *IEEE Ind. Electron. Mag.*, vol. 7, no. 4, pp. 42–55, Dec. 2013.

[3] J. Guerrero *et al.*, "Control strategy for flexible microgrid based on parallel line-interactive ups systems," *IEEE Trans. Ind. Electron.*, vol. 56, no. 3, pp. 726–736, Mar. 2009.

[4] S. Cady, A. Domínguez-García, and C. Hadjicostis, "A distributed generation control architecture for islanded ac microgrids," *IEEE Trans. Control Syst. Technol.*, vol. 23, no. 5, pp. 1717–1735, 2015.

[5] J. Simpson-Porco, F. Dörfler, and F. Bullo, "Synchronization and power sharing for droop-controlled inverters in islanded microgrids," *Automatica*, vol. 49, no. 9, pp. 2603–2611, 2013.

[6] A. Bidram *et al.*, "Frequency control of electric power microgrids using distributed cooperative control of multi-agent systems," in *Proc. IEEE Conf. Cyber Technol. in Automat., Control and Intell. Syst.*, May 2013, pp. 223–228.

[7] Q. Shafiee, J. Guerrero, and J. Vasquez, "Distributed secondary control for islanded microgrids - a novel approach," *IEEE Trans. Power Electron.*, vol. 29, no. 2, pp. 1018–1031, Feb. 2014.

[8] J. Schiffer, R. Ortega, A. Astolfi, J. Raisch, and T. Sezi, "Conditions for stability of droop-controlled inverter-based microgrids," *Automatica*, vol. 50, no. 10, pp. 2457–2469, 2014.

[9] S. Trip, M. Bürger, and C. De Persis, "An internal model approach to (optimal) frequency regulation in power grids with time-varying voltages," *Automatica*, vol. 64, pp. 240–253, 2016.

[10] J. Driesen and K. Visscher, "Virtual synchronous generators," in *Proc. IEEE Power and Energy Soc. Gen. Meeting*, Jul. 2008, pp. 1–3.

[11] K. Sakimoto *et al.*, "Stabilization of a power system with a distributed generator by a virtual synchronous generator function," in *Proc. IEEE Int. Conf. Power Electron.*, May 2011, pp. 1498–1505.

[12] F. Dörfler, M. Chertkov, and F. Bullo, "Synchronization in complex oscillator networks and smart grids," *Proc. Natl. Acad. Sci. U.S.A.*, vol. 110, no. 6, pp. 2005–2010, 2013.

[13] M. Zholbaryssov and A. Domínguez-García, "Exploiting phase cohesiveness for frequency control of islanded inverter-based microgrids," accepted to IEEE Conf. Decision and Control, Dec. 2016.

[14] F. Dorfler, J. Simpson-Porco, and F. Bullo, "Breaking the hierarchy: Distributed control and economic optimality in microgrids," *IEEE Trans. Control Network Syst.*, vol. 3, no. 3, pp. 241–253, 2016.

[15] A. Bergen and V. Vittal, *Power systems analysis*. Prentice Hall, 2000.

[16] H. Han, X. Hou, J. Yang, J. Wu, M. Su, and J. M. Guerrero, "Review of power sharing control strategies for islanding operation of ac microgrids," *IEEE Trans. Smart Grid*, vol. 7, no. 1, pp. 200–215, Jan. 2016.

[17] L. Luo and S. Dhople, "Spatiotemporal model reduction of inverter-based islanded microgrids," *IEEE Trans. Energy Conversion*, vol. 29, no. 4, pp. 823–832, 2014.

[18] J. Schiffer, D. Zonetti, R. Ortega, A. Stanković, T. Sezi, and J. Raisch, "A survey on modeling of microgrids—from fundamental physics to phasors and voltage sources," *Automatica*, vol. 74, pp. 135–150, 2016.

[19] M. Chandorkar, D. Divan, and R. Adapa, "Control of parallel connected inverters in standalone ac supply systems," *IEEE Trans. Ind. Appl.*, vol. 29, no. 1, pp. 136–143, Jan. 1993.

[20] K. De Brabandere, B. Bolsens, J. Van den Keybus, A. Woyte, J. Driesen, and R. Belmans, "A voltage and frequency droop control method for parallel inverters," *IEEE Trans. Power Electron.*, vol. 22, no. 4, pp. 1107–1115, 2007.

[21] N. Pogaku, M. Prodanovic, and T. C. Green, "Modeling, analysis and testing of autonomous operation of an inverter-based microgrid," *IEEE Trans. Power Electron.*, vol. 22, no. 2, pp. 613–625, Mar. 2007.

[22] I. A. Hiskens and D. J. Hill, "Energy functions, transient stability and voltage behaviour in power systems with nonlinear loads," *IEEE Trans. Power Syst.*, vol. 4, no. 4, pp. 1525–1533, Nov 1989.

[23] A. Araposthatis *et al.*, "Analysis of power-flow equation," *Int. J. Elect. Power & Energy Syst.*, vol. 3, no. 3, pp. 115 – 126, 1981.

[24] R. A. Horn and C. R. Johnson, *Matrix Analysis*, 2nd ed. Cambridge University Press, 2013.

[25] D. P. Bertsekas and J. N. Tsitsiklis, *Parallel and Distributed Computation: Numerical Methods*. Prentice Hall, 1989.

[26] S. Boyd and L. Vandenberghe, *Convex optimization*. Cambridge university press, 2004.

[27] Å. Björck, *Numerical Methods for Least Squares Problems*. Society for Industrial and Applied Mathematics, 1996.

[28] C. Lawson and R. Hanson, *Solving Least Squares Problems*. Society for Industrial and Applied Mathematics, 1995.

[29] J. F. Mota *et al.*, "A proof of convergence for the alternating direction method of multipliers applied to polyhedral-constrained functions," *arXiv preprint arXiv:1112.2295*, 2011.

[30] V. Yadav and M. V. Salapaka, "Distributed protocol for determining when averaging consensus is reached," in *45th Annual Allerton Conference*, 2007, pp. 715–720.

ACKNOWLEDGEMENTS

This work was supported in part by the National Science Foundation (NSF) under grant ECCS-CPS-1135598, and by the US Department of Energy (DOE) GEARED Initiative under grant DE-0006341.

Madi Zholbaryssov (S'16) received the B.S. degree in electrical engineering in 2011 and the M.S. degree in electrical engineering in 2014, both from the University of Illinois at Urbana-Champaign, Urbana, IL, USA, where he is currently pursuing the Ph.D.degree in electrical engineering.

His current research interests include distributed control, distributed optimization and their application to electric power systems.

Alejandro D. Domínguez-García (S'02, M'07) received the degree of Electrical Engineer from the University of Oviedo (Spain) in 2001 and the Ph.D. degree in electrical engineering and computer science from the Massachusetts Institute of Technology, Cambridge, MA, in 2007.

He is an Associate Professor with the Department of Electrical and Computer Engineering (ECE), and a Research Associate Professor with the Coordinated Science Laboratory and the Information Trust Institute, all at the University of Illinois at Urbana-Champaign. He is affiliated with the ECE Power and Energy Systems area, and has been a Grainger Associate since August 2011.

His research interests are in the areas of system reliability theory and control, and their applications to electric power systems, power electronics, and embedded electronic systems for safety-critical/fault-tolerant aircraft, aerospace, and automotive applications.

Dr. Domínguez-García received the NSF CAREER Award in 2010, and the Young Engineer Award from the IEEE Power and Energy Society in 2012. In 2014, he was invited by the National Academy of Engineering to attend the US Frontiers of Engineering Symposium, and was selected by the University of Illinois at Urbana-Champaign Provost to receive a Distinguished Promotion Award. In 2015, he received the U of I College of Engineering Dean's Award for Excellence in Research. He is an editor of the IEEE Transactions on Power Systems and IEEE Power Engineering Letters.